Theoretical study of the vibrational edge modes in graphene nanoribbons

M. Vandescuren,[1,*] P. Hermet,[1] V. Meunier,[2] L. Henrard,[1] and Ph. Lambin[1]
[1]*Laboratoire de Physique du Solide, Facultés Universitaires Notre-Dame de la Paix, 5000 Namur, Belgium*
[2]*Computer Science and Mathematics Division, Oak Ridge National Laboratory, Oak Ridge, Tennessee 37831, USA*
(Received 25 June 2008; revised manuscript received 2 September 2008; published 4 November 2008)

We investigate the phonon normal modes in hydrogen-terminated graphene nanoribbons (GNRs) using the second-generation reactive empirical bond order (REBOII) potential and density-functional theory calculations. We show that specific modes, absent in pristine graphene and localized at the GNR edges, are intrinsic signatures of the vibrational density of states of the GNRs. Three particular modes are described in details: a transverse phonon mode related to armchair GNRs, a hydrogen out-of-plane mode present in both armchair and zigzag GNRs, and the Raman radial-breathing-like mode. The good agreement between the frequencies of selected edge modes obtained using REBOII and first-principles methods shows the reliability of this empirical potential for the calculation and the assignment of phonon modes in carbon nanostructures where carbon atoms present a sp^2 hybridization.

DOI: 10.1103/PhysRevB.78.195401 PACS number(s): 61.46.−w, 63.20.Pw

I. INTRODUCTION

Graphite nanocrystallites are the most recently discovered carbon-based nanomaterials.[1] These nanoflakes are a few atoms thick, are stable under ambient conditions, and have a lot of promises as nanoscale transistors.[2] Their remarkable properties make their study one of the hottest subjects in present-day nanoscience.[3]

Graphene nanoribbons (GNRs) are similar to carbon nanotubes as they are prototypical one-dimensional (1D) nanostructures. It has been recently shown that a GNR can be peeled off from the topmost layer of highly oriented pyrolytic graphite by scanning tunneling microscope (STM) lithography operated in air, allowing the design of arbitrary geometry.[4] Because of the presence of edges on both sides, GNRs possess a set of particular properties, depending on width and helicity. Many investigations so far have focused their attention on the electronic and magnetic properties of GNRs, revealing spectacular effects arising from the confinement of electron and hole gases.[5–8] One of the most remarkable findings is that electrons and holes can be specularly reflected, such as billiard particles, at the edges of a graphene ribbon.[9]

Electronic states localized at zigzag edges of a graphene sheet[10] by increasing the local electronic density of states at the Fermi level can induce superconductivity confined along the edges.[11] An important issue for modeling this behavior is related to the availability of an appropriate vibrational model for the description of the phonon-mediated Cooper pairing mechanism. Like electrons, phonons can be localized at the edges of a ribbon, which could enhance the electron-phonon interactions and further contribute to edge superconductivity. Despite this specific interest, only a few works have been devoted to the study of the vibrational structure of GNRs. A transverse-optical edge mode typical to armchair GNRs (nanoribbon with armchair edges) has been predicted theoretically[12] and detected experimentally a few years later.[13] This type of mode has further been investigated in GNRs with various widths[14] using the first-generation reactive empirical bond order potential (REBO).[15] In a recent work on Raman-active mode in GNRs, Zhou *et al.*[16] studied vibrational properties within the density-function theory (DFT) framework, providing *ab initio* prediction of special GNRs modes. At last, a systematic study of phonon dispersions of GNRs was carried out by Yamada *et al.*[17] by using a transferable force field model and the zone folding method.

The main objective of this work is to study and characterize the intrinsic phonon modes of GNRs [i.e., modes which are not present in two-dimensional (2D) graphene]. For this purpose, we used the second-generation reactive empirical bond order (REBOII) potential[18] to calculate the phonon modes of different GNRs. By construction, this force field reproduces with a good accuracy the static and dynamical properties of pure graphene, pure diamond, and usual forms of hydrocarbon molecules.[19] However, there is not much information available about the reliability of REBOII potential for dynamical properties of carboneous materials. Thus, first-principles calculations of phonon mode frequencies of different GNRs have been also performed to state the reliability of the potential by direct comparison between the REBOII frequencies and the DFT ones. This potential constitutes an interesting alternative to first-principles methods to compute, at low computational efforts, the phonons modes in GNRs. Studying phonons within REBOII force field is therefore a step forward for its validation as a reliable potential in hydrocarbon structure with sp^2 conformation.

II. METHODOLOGY AND COMPUTATIONAL DETAILS

The local vibrational density of state (lVDOS) on an atomic site i is given for a frequency ω by

$$\rho_i(\omega) = 2\omega \sum_{\nu} \sum_{\alpha} |u_{i,\nu}(\alpha)|^2 \delta(\omega^2 - \omega_\nu^2), \tag{1}$$

where the sums run over all the modes ν and the space directions α. ω_ν and $u_{i,\nu}(\alpha)$ are the frequency and the (i,α) component of the νth phonon eigenvector, respectively. They are calculated by means of the lattice-dynamics equations

$$\sum_{j,\beta} D_{ij}(\alpha,\beta)u_{j,\nu}(\beta) = \omega_\nu^2 u_{i,\nu}(\alpha), \tag{2}$$

where β denote the Cartesian directions and $\tilde{D}$ is the dynamical matrix defined by

$$D_{ij}(\alpha,\beta) = \frac{\phi_{ij}(\alpha,\beta)}{\sqrt{M_i M_j}}. \tag{3}$$

M are the masses of atoms and ϕ_{ij} is the second-rank force-constant tensor containing the complete information about the interactions between the ith and the jth atoms. The total VDOS is therefore calculated from the lVDOS by summing $\rho_i(\omega)$ in Eq. (1) over all the atomic sites of the structure. From Eq. (3), it is obvious that the force-constant tensors are the central quantities to be determined in order to compute the lVDOS. These tensors are calculated using both first-principles approach and the empirical REBOII potential for comparison purposes.

A. First-principles calculations

DFT calculations were performed with the SIESTA package[20] on three different armchair and zigzag GNR widths [N=4, 10 and 15, where N labels the number of atoms across the GNR width (see Fig. 2 in the case of N=10 armchair GNR, for instance)]. These GNRs have been chosen to provide a reliable comparison basis with REBOII results. Exchange-correlation effects were handled within the local-density approximation (LDA) as proposed by Perdew and Zunger.[21] Core electrons are replaced by nonlocal norm-conserving pseudopotentials.[22] The valence electrons were described by localized pseudoatomic orbitals with a double-ζ singly polarized (DZP) basis set.[23] The cut-off radii for the s and p orbitals were, respectively, 5.12 and 6.25 a.u. for the carbon atoms and 6.05 a.u. for the hydrogen atoms. The first Brillouin zone was sampled according to the Monkhorst-Pack scheme[24] by using a $30\times1\times1$ k-points grid for the insulator GNRs, whereas a $60\times1\times1$ k-points grid was used for the metallic ones. The atomic positions in the unit cell of each GNRs were relaxed at fixed lattice parameters using a conjugate gradient until the maximum residual force on the atoms was smaller than 1×10^{-3} eV/Å. Real-space integration was performed on a regular grid corresponding to a plane-wave cutoff around 300 Ry, for which the structural relaxations and phonons are fully converged. Dynamical matrix was calculated at the Γ-point in the harmonic approximation via the knowledge of the Hellmann-Feynman (HF) forces by using the *direct method*[25] and an atomic displacement of 0.03 Å as detailed in Ref. 26. Positive and negative displacements were used to minimize numerical errors in the HF calculations related to anharmonic effects. Finally, zone-center phonon modes were calculated by a direct diagonalization of the dynamical matrix.[27]

B. Force-field calculations

The empirical REBOII potential is the second generation of pairwise-like potential for (hydro)carbon materials based on the classical model initially proposed by Tersoff for silicon[28] and further adapted to carbon materials.[15,29] Briefly stated, the total energy for solid carbon materials and hydrocarbon molecules is expressed by

$$E = \sum_i \sum_{j>i} f_c(r_{ij})[V_R(r_{ij}) - b_{ij}V_A(r_{ij})], \tag{4}$$

where $f_c(r)$ is a cut-off-distance function. V_R and V_A are, respectively, the repulsive and attractive parts of the potential. The coefficient b_{ij} depends on the angles between the bond ij and all the bonds issued from the sites i and j. The parameters of the potential depend on the local coordination (3 for graphite and 4 for diamond). Numerous calculations have already demonstrated the validity of this potential when addressing structural properties of graphitic systems, including fullerenes and nanotubes, and nanodiamonds.[19] The advantage of this model over *ab initio* approaches is its ease of implementation, its low computational cost, and therefore its ability to tackle large and complex structures. Also, the first version of the REBO potential[15] has already been used for both phonon studies and thermal properties of carbon nanostructures, yielding good agreement with first-principles results.[14] Even if much less is known on the reliability of REBOII for dynamical properties of carboneous materials, we can rely on the significant improvements of REBO in terms of bond energy, bond-lengths, and force-constants calculations[18] to yield an accurate prediction of phonon modes in hydrocarbon materials.

This empirical force field has been used to optimize the atomic positions of different GNRs and to compute their interatomic force-constant tensors. A conjugate gradient algorithm was used to perform the optimization of the atomic positions until the energy of the system reached its minimum with a precision of 1×10^{-5} eV. The optimized C-H bonds were slightly longer than the 1.09 Å, and the C-C bond lengths were about 1.42 Å, except for the edges carbons where the bond lengths were closer to 1.41 Å. These optimized bond lengths are in good agreement with the ones reported for hydrocarbon structures in sp^2 configuration. The interatomic force-constant tensors were calculated for each C-C or C-H interaction within the harmonic approximation. We used the finite difference method on the total energy with an atomic displacement of 1×10^{-3} Å. The force constants are calculated up to the fourth neighbors which is the lowest-order interaction required to have a reliable representation of the dynamics of hydrocarbon structures.[30]

The usual method to calculate the lVDOS (and therefore the VDOS) spectrum consists of injecting in Eq. (1) the values of ω_ν and $u_{i,\nu}(\alpha)$ obtained by direct diagonalization of the dynamical matrix of the system [Eq. (2)]. By contrast, the spectral moments method based on a recursive technique similar to the ones initially developed by Lanczos[31] to determine the eigenvalues of large matrices allows the lVDOS computation of very large harmonic systems to be directly computed without any diagonalization of the dynamical matrix. The mode frequencies in the lVDOS spectra are then directly obtained from the position of the peaks in the calculated lVDOS spectra.[32,33] The mathematical details of the spectral moments method can be found in Refs. 34–36.

We have used the spectral moments method on a $50\times1\times1$ supercell to compute the VDOS spectra of the different GNRs displayed in this paper. A direct diagonalization of the dynamical matrix calculated using the REBOII force field was also used to compare very accurately the REBOII phonon frequencies of the different GNRs calculated with the DFT ones at the Γ-point.

III. RESULTS AND DISCUSSION

Two main complementary methods exist to assign the edge-localized phonon modes involved in a GNR. The first method is the most standard and has already been used by the authors of Refs. 12 and 14. It consists in the comparison of the phonon band structure of GNRs and that of the graphene sheet. The phonon branches which are not involved in the 1D projected dispersion relation of the 2D graphene sheet are therefore assigned to GNRs. The second method compares the VDOS spectra of GNRs and that of the graphene sheet. Because edge-localized phonon modes are absent in graphene, characteristic modes of GNRs are expected to be detected in the differences between the VDOS spectra of GNRs and perfect graphene. To the best of our knowledge, this method has never been used for the investigation of the edge-localized phonon modes. Its main limitation is that peaks only appear in the VDOS spectra when their dispersion curves are flat in the first Brillouin zone. These two methods are therefore complementary because if a specific mode turns out to be located in the continuum region of the graphene band structure, it will remain undetectable within the first method. In this work, we have used the VDOS method to investigate the edge-localized phonon modes involved in a GNR to complete the information obtained by the authors of Refs. 12 and 14 using the band-structure method.

A. Edge-localized phonon modes in GNRs

1. Transverse phonon modes in armchair GNRs

Figure 1 compares the VDOS calculated with the empirical REBOII potential between a graphene sheet and three armchair GNRs of different widths (N=5, 15, and 25).[37] We observe two phonon modes located around 365 and 858 cm^{-1} present in all GNRs and absent in the VDOS of graphene. To ensure that real edge phonon modes are selected, much attention has been paid to avoid Van Hove singularities. These singular peaks are often tall in small GNR widths, whereas they nearly disappeared in larger ones. In addition, edge-localized phonon modes have peaks of approximately constant height in the lVDOS of atoms localized at the edges in all GNRs. Keeping that in mind helps us in the detection of edge-localized phonon modes and convinces us that the 365 and 858 cm^{-1} modes are characteristic to armchair GNRs. The real-space representation of the phonon eigendisplacement vectors of these two modes allows us to assign the mode calculated at 365 cm^{-1} to an out-of-plane edge-localized motion of the carbon atoms (see Fig. 2). The mode localized at 858 cm^{-1} has been assigned to an out-of-plane edge-localized motion of the hydrogens (see Fig. 3).

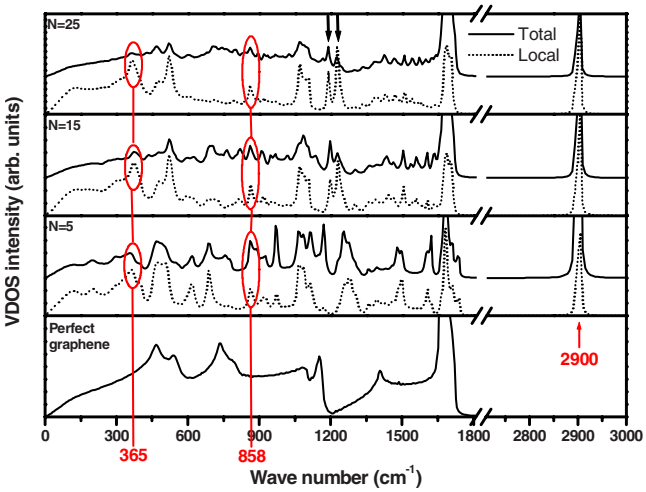

FIG. 1. (Color online) Calculated (using the empirical REBOII potential) vibrational densities of states of a perfect graphene sheet and three different armchair GNRs of widths N=5, 15, and 25, respectively. The solid curves are the total VDOS. The dotted curves are lVDOS calculated on a carbon site close to a hydrogen of the edge. The C-H stretching mode is located at 2900 cm^{-1} and two edge-localized phonon modes characteristic to the armchair GNRs are centered around 365 and 858 cm^{-1}. The arrows mark the position of two shear modes of the ribbon.

This latter mode will be further discussed in this paper.

In literature, Yamamoto *et al.*[14] calculated the phonon band structures of graphene and armchair GNRs without hydrogens at the edges using the empirical REBO potential. They observed only one edge mode centered at 430 cm^{-1} (similar to ours at 365 cm^{-1}) which is upshifted due to the lower effective mass resulting from the absence of hydrogen at the edges. A rigorous analysis based on the diagonalization of the dynamical matrix[38] for the three armchair GNRs shows that the peak located around 365 cm^{-1} is actually a doublet with its two components centered at 356 (A) and 362 cm^{-1} (S) for N=4. Here, S and A, respectively, denote the symmetric and antisymmetric modes involved in the doublet. We observe that the splitting between these two frequencies decreases [358 (A) and 367 cm^{-1} (S)] when the armchair GNR width increases (N=10) and the symmetric

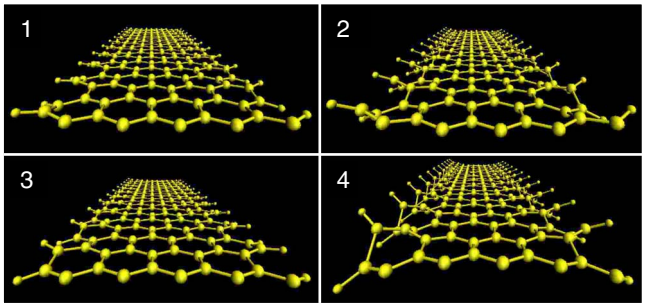

FIG. 2. (Color online) Four snapshots displaying the 365 cm^{-1} edge-localized phonon mode at the Γ-point of a N=10 armchair GNR saturated with hydrogens. The sequence order is indicated on the upper left corner of each picture. N=10 represents the number of carbon atoms across the width.

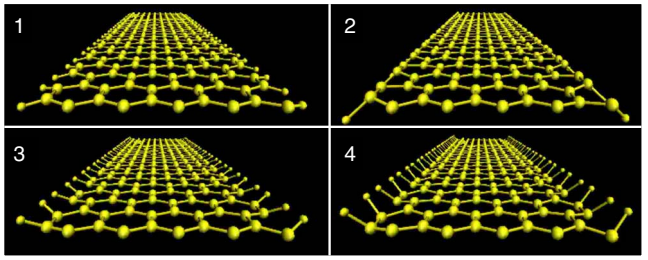

FIG. 3. (Color online) Four snapshots displaying the 858 cm^{-1} edge-localized phonon mode at the Γ-point of a $N=10$ armchair GNR saturated with hydrogens. The sequence order is indicated on the upper left corner of each picture.

and antisymmetric modes are degenerated at 368 cm^{-1} for $N=15$. The same behavior is reproduced by our DFT calculations with phonon modes centered at 370 (A) and 405 cm^{-1} (S) for $N=4$, 376 cm^{-1} (A and S) for $N=10$, and 376 cm^{-1} (A and S) for $N=15$. Although the frequencies of the tranverse phonon mode calculated with the REBOII potential in armchair GNRs are always underestimated with respect to the DFT ones, they are in good agreement and the largest discrepancy between the two models is less than 6%.

2. Hydrogen edge-localized phonon modes in zigzag GNRs

Figure 4 compares the VDOS calculated with the empirical REBOII potential between a graphene sheet and three different zigzag GNRs widths ($N=5$, 10, and 20). By contrast to the armchair GNRs, the transverse phonon edge-localized mode has no equivalent in zigzag GNRs in the same frequency range. At higher frequencies, however, we observe a characteristic zigzag GNR mode centered around

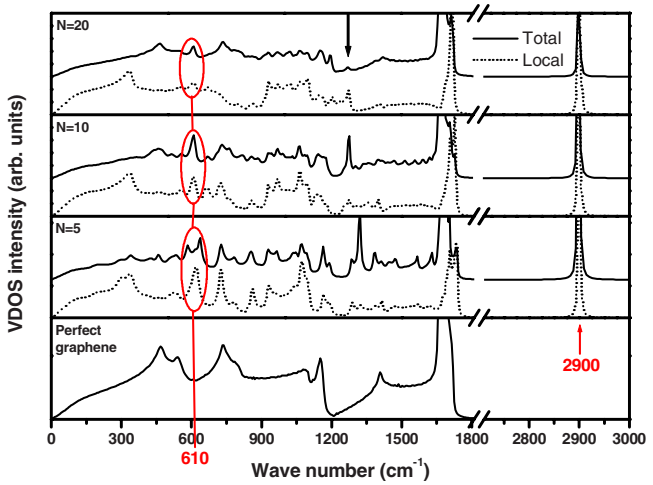

FIG. 4. (Color online) Comparison between the calculated VDOS of a perfect graphene sheet and three different zigzag GNR widths ($N=5$, 10, and 20) using the empirical REBOII potential. The solid curves are the total VDOS and the dotted curves are lVDOS on a carbon near to a hydrogen of the edge. The C-H stretching mode is located at 2900 cm^{-1} and the only edge-localized phonon mode characteristic to the zigzag GNRs lies around 610 cm^{-1}. The arrow marks the position of an *in-plane* hydrogen edge phonon.

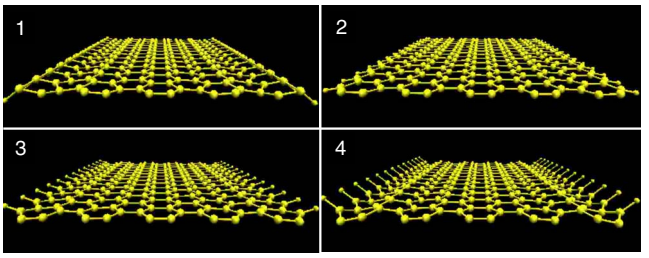

FIG. 5. (Color online) Four snapshots displaying the 610 cm^{-1} edge-localized phonon mode at the Γ-point of a $N=10$ zigzag GNR saturated with hydrogens. The sequence order is indicated on the upper left corner of each picture.

610 cm^{-1}. This phonon mode (displayed in Fig. 5) has been assigned to an out-of-plane edge-localized mode of the hydrogens. Additional calculations performed on hydrogen-free edges indicate that this mode does not appear in the VDOS spectra.

Figure 6 shows the oscillation amplitude of the hydrogen edge phonon mode for $N=10$ zigzag GNR (curves with circles) with respect to the distance from the edge of the ribbon. The oscillation amplitudes of the carbons are normalized by the amplitude of the hydrogen of the edge. Same curves are obtained for GNRs with larger widths, which indicate that the central part of the ribbons does not participate to the mode for width exceeding about 30 Å. Thus, for an infinite GNR (the perfect graphene sheet), the carbon atoms no longer oscillate. This mode located at 610 cm^{-1} is therefore intrinsic to zigzag GNRs.

In addition, this hydrogen edge mode splits into two peaks centered at 585 and 635 cm^{-1} in the total VDOS displayed in Fig. 4 for $N=5$. These two peaks are, respectively, as-

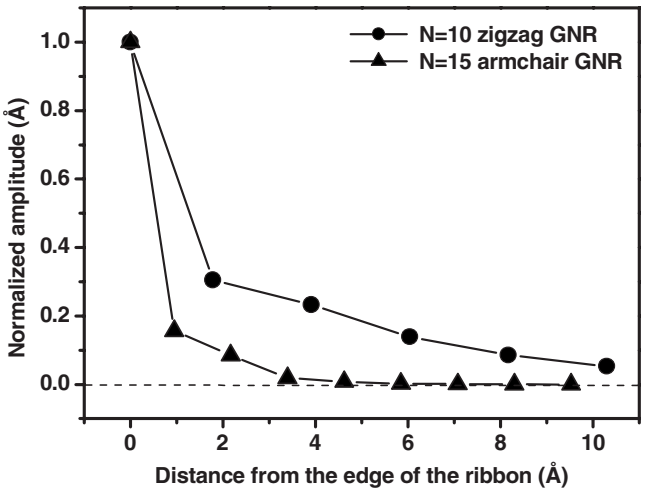

FIG. 6. Normalized amplitudes of atomic oscillations of the two hydrogen edge modes. The $N=10$ zigzag GNR mode centered at 610 cm^{-1} is represented with circles and the $N=15$ armchair GNR mode centered at 858 cm^{-1} with triangles. Both ribbons are approximately 20 Å wide. The x axis represents the distance from the edge of the ribbon (i.e., the amplitude at the middle of the ribbon is represented on the last point of the curve). Only the largest amplitudes of the carbon atoms are represented. The lines are guides for the reader's eyes.

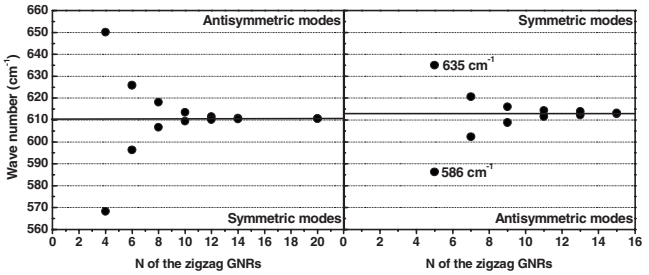

FIG. 7. Calculated frequencies using REBOII potential of the symmetric (S) and antisymmetric (A) modes of zigzag GNRs for N even (left-hand graph) and N odd (right-hand graph). As the width of the ribbon decreases, the splitting between S and A increases. The modes converge to 613 cm^{-1} for odd N and to 611 cm^{-1} for even N as N becomes infinitely large.

signed to antisymmetric (both edges oscillate with opposite phases) and symmetric (both edges oscillate in phase) modes. A systematic study has been carried out for different zigzag GNR widths varying from 4 to 15 to characterize these two particular modes. The results are reported in Fig. 7 and can be separated into two groups: those obtained for odd N and those obtained for even N. We observe that the frequency of the symmetric (antisymmetric) mode increases (decreases) when N increases while being even (odd). For a given GNR, the frequency splitting between symmetric and antisymmetric modes is due to vibrational interferences between both edges. Indeed, for a fixed width and depending on the selected mode (symmetric or antisymmetric), the interferences are either constructive or destructive making the frequency slightly higher or lower than the asymptotic value. In Fig. 6, the nonzero amplitude in the middle of the ribbon indicates that some interactions between both edges are still active, leading to an estimate of the localization length of the edge phonon (around 10 Å). Now, supposing that the width of the GNR becomes larger and larger, no more interferences would take place at the center of the ribbon and the frequencies of the symmetric and antisymmetric modes therefore converge to the limiting value (see Fig. 7). Thus, the modes converge either to 613 cm^{-1} for N odd or to 611 cm^{-1} for N even when N goes to infinity. The difference (2 cm^{-1}) between these asymptotic values is not significant.

The frequency of the symmetric and antisymmetric hydrogen edge phonon has also been calculated by using DFT for three different zigzag GNRs widths (N=4, 10, and 15) and are reported in Table I (the first three lines) together with the REBOII ones. The frequencies calculated by both models are found to be in close agreement; the largest discrepancy being less than 4%. Thus, the REBOII potential is reliable for the prediction of this type of edge mode in zigzag GNRs.

3. Hydrogen edge-localized phonon modes in armchair GNRs

The same systematic study has been performed for the armchair GNRs with edges saturated with hydrogens. As previously mentioned, out-of-plane edge-localized phonons of hydrogen atoms have been observed around 858 cm^{-1} in the VDOS spectra of Fig. 1 for N=5, 15, and 25 armchair GNRs. Through the direct diagonalization of the dynamical matrix, we observed that this mode is a doublet (symmetric and antisymmetric) for all armchair GNRs with widths varying from N=5 to 29. As they are degenerated, except for N=4 (860 and 863 cm^{-1}) and N=3 (842 and 863 cm^{-1}), the hydrogen edge phonon modes are more strongly localized at the edges of the armchair GNRs than those for the zigzag ones. This observation is highlighted in Fig. 6 showing the normalized oscillation amplitude of the hydrogen edge phonon for N=15 as a function of the distance from the edge of the GNR. Since this curve is common to all armchair width, it is obvious that the oscillation amplitudes decrease more rapidly for armchair than for zigzag GNRs. Therefore no interference between both edges can take place at the center of the ribbon except for very small armchair GNR widths (N=4 and 3).

The frequencies of the symmetric and antisymmetric hydrogen edge phonons have also been calculated by using DFT for three different armchair GNRs with widths N=4, 10, and 15. They are reported in Table I with those calculated by the REBOII potential. Although the frequency relative difference calculated by both models is greater for the armchair GNRs than for the zigzag ones, their agreement is accurate enough for a reliable prediction of this type of edge mode in armchair GNRs; the largest discrepancy being less than 10%.

4. Other ribbon modes calculated with the REBOII potential

In zigzag GNRs, the signature of an *in-plane* hydrogen mode localized at the edges and centered around 1275 cm^{-1}

TABLE I. Comparison between the Γ-point frequencies (in cm^{-1}) of the hydrogen edge mode calculated with the REBOII potential and DFT for zigzag (N_{zz}) and armchair (N_{ar}) GNRs of different widths. The errors (in percent) are shown in the right-most column.

	Symmetric modes			Antisymmetric modes		
Structures	REBOII	DFT	Errors	REBOII	DFT	Errors
N_{zz}=4	560	544	2.9	650	662	1.8
N_{zz}=10	609	589	3.4	613	602	1.8
N_{zz}=15	613	598	2.6	613	596	2.9
N_{ar}=4	864	797	8.4	860	786	9.4
N_{ar}=10	858	793	8.2	858	792	8.3
N_{ar}=15	858	797	7.7	858	795	7.9

TABLE II. Comparison between the RBLM frequencies (in cm^{-1}) of armchair (N_{ar}) and zigzag (N_{zz}) GNRs within DFT (from Ref. 16) and REBOII (this work) frameworks. The errors (in percent) are also indicated. Our DFT results are shown between brackets in the DFT column when available.

N_{ar}	DFT	REBOII	Errors	N_{zz}	DFT	REBOII	Errors
4	661 [668]	637	3.72	4	406 [407]	375	7.68
5	543	521	4.07	5	330	301	8.96
6	466	436	6.31	6	278	252	9.18
7	403	378	6.28	7	238	217	9.06
8	354	328	7.34	8	210	190	9.53
9	319	296	7.03	9	187	169	9.82
10	288 [289]	266	7.67	10	169 [168]	152	9.95
11	262	244	7.01	11	153	138	9.69
12	242	223	7.69	12	141	128	9.01

can be observed in the VDOS of Fig. 4 (see the arrow). The hydrogen atoms oscillate at constant distance of the edges carbons (arc of a circle).

In addition to the edge-localized modes discussed here above, other peaks appear in the VDOS of the ribbons and not in graphene. For instance, the peaks around 1190 and 1230 cm^{-1} in armchair GNRs (arrows in Fig. 1) are shear modes of the ribbon with polarization parallel to the free edges. Their amplitudes are important everywhere across the width.

B. Radial-breathing-like mode in GNRs

Among the characteristic phonon modes in the GNRs, the calculation of the radial-breathing-like mode (RBLM) is undoubtedly the best way to ascertain the validity of the REBOII potential with respect to first-principles methods. Indeed, (i) this mode exists in all GNRs and (ii) the frequency of this mode decreases when the GNR width increases in linear proportion to the inverse square root of the width.[16] By contrast with the previous ribbon modes, the RBLM does not give rise to a peak in the VDOS due to its important dispersion. The diagonalization of the dynamical matrix is therefore mandatory for studying this phonon mode. The RBLM is an in-plane mode where the atoms of the structure oscillate perpendicularly to the edges. The amplitudes increase as we consider atoms closer and closer to the edge of the ribbon. The atoms at the center do not move at all.

Table II reports the RBLM frequencies at the Γ-point of different GNRs calculated by using DFT and the REBOII potential. In a recent article, Zhou *et al.*[16] calculated the RBLM on nine different H-terminated armchair and zigzag GNRs (N varying from 4 to 12) from DFT-based methods using plane waves, LDA, and the projector augmented-waves formalism as implemented in the VASP code. The DFT frequencies obtained by these authors are also reported in Table II and complete our data. We observe a very good agreement between our calculated DFT frequencies and those from Zhou *et al.*, showing the good accuracy of our pseudopotentials and orbital-localized basis sets. In addition, the deviation of the RBLM frequencies obtained with REBOII is smaller than 10% with respect to the DFT ones and becomes roughly constant for the wider GNRs, highlighting the transferability of the empirical REBOII potential for all the GNRs.

Panel A of Fig. 8 displays the linear fit of the RBLM frequencies (ω) calculated using DFT and the REBOII potential as a function of the inverse of the square root of the GNR width (W).[39] The fitting formula used is given by

$$\omega = a\frac{1}{\sqrt{W}} + b, \tag{5}$$

where a and b are the two-dimensional constants. The linear fit gives the parameters $a=1606.1$ cm^{-1} $Å^{1/2}$ and $b=-214.7$ cm^{-1} for the REBOII model, whereas the parameters $a=1667.9$ cm^{-1} $Å^{1/2}$ and $b=-210.2$ cm^{-1} are obtained for the DFT frequencies. These two sets of parameters are in agreement with those reported in Ref. 16. In a recent paper, Yamada *et al.*[17] calculated the phonon dispersions of GNRs using a force-field model. Their RBLM frequencies at the Γ-point are displayed in the panel B of Fig. 8. We observe that the frequencies reported by these authors are close to the

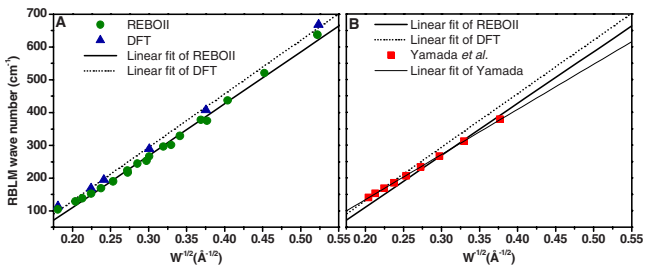

FIG. 8. (Color online) A: Linear fit (solid line) of the RBLM frequencies (full circles) as a function of the inverse of the square root of the GNR width. The C-H bonds are not included in the calculation of the width of ribbons. The triangles represent our DFT results and the dotted line represents the linear fit. B: The linear fits of the RBLM frequencies of the REBOII and the DFT are, respectively, the dotted and the full lines. The squares represent RBLM frequencies from Yamada *et al.* (Ref. 17). A linear fit is displayed on the figure by the thin straight line. Results from Yamada *et al.* (Ref. 17) are separated from DFT and REBOII ones for presentation purpose.

DFT ones for large nanoribbons but deviate from the DFT straight line when the width of the GNR decreases. Although there are not enough data to perform an accurate comparison, these results show how nice an empirical model can fit DFT calculations.

Finally, since the REBOII frequencies are always lower than the DFT ones, a scaling factor (γ) can be applied to the REBOII frequencies ($\omega^k_{\mathrm{REBOII}}$) to improve their agreement with the DFT ones (ω^k_{DFT}). This scaling factor was calculated by minimizing the relative error Δ defined as

$$\Delta(\gamma) = \sqrt{\frac{\sum_k (\omega^k_{\mathrm{DFT}} - \gamma\omega^k_{\mathrm{REBOII}})^2}{\sum_k (\gamma\omega^k_{\mathrm{REBOII}})^2}}, \tag{6}$$

where the sums are over all the GNR structures considered in Table II. The minimization of Eq. (6) provides a scaling factor $\gamma = 1.07$ with an error (Δ) of 2.2%. After this simple correction, the REBOII potential can predict with a better accuracy the frequencies of the RBLM mode, expectedly for all ribbon geometries (with zigzag, armchair, or chiral edges).

IV. CONCLUSIONS

In this work, we have investigated the intrinsic phonon modes of GNRs (i.e., modes which are absent in pristine graphene sheets) by using the REBOII force-field and first-principles methods. While phonons are extremely sensitive to the used potential, the comparison between the REBOII frequencies and the DFT ones indicates that this force field is well suited for an accurate determination of phonon modes in sp^2 bonded systems such as graphitic nanoribbons. The largest relative difference between the calculated frequencies obtained within these two models is less than 10%.

Three modes have been studied in details in this paper. The first one already discovered in dispersion relations calculated by Yamamoto *et al.*[14] is an edge mode existing only in armchair GNRs. The second one is a hydrogen mode appearing in our VDOS exclusively in zigzag and armchair GNRs saturated with hydrogens. The last one brought out in a theoretical work by Zhou *et al.*[16] on Raman-active modes in GNRs is the Raman radial-breathing-like mode. For this latter mode, we have also calculated that a scaling factor of 1.07 improves the agreement between the calculated RBLM frequencies obtained within the REBOII force field and the DFT ones.

Finally, we think that the computational strategy proposed in this work, using the REBOII force field and the spectral moment method coupling, will be a step forward in the future for the investigation of defects phonon modes in carbon nanotubes. Indeed, these materials constitute a challenge for first-principles methods due to their important number of atoms. In addition, the dimension of their dynamical matrices is very large and the standard diagonalization methods fail or require long computational time to determine their eigenvalues and eigenvectors.

ACKNOWLEDGMENTS

M.V. and L.H. are supported by the Belgian National Fund for Scientific Research (FNRS). P.H. is supported by the European Commission under the 6 Framework Programme (STREP project BNC tubes under Contract No. NMP4-CT-2006-0335D). A portion of this research was sponsored by the Scientific User Facilities Division, Office of Basic Energy Sciences, U. S. Department of Energy. The authors acknowledge the use of the Namur Interuniversity Scientific Computing Facility (Namur-ISCF), a common project between FNRS, SUN Microsystems, and Les Facultés Universitaires Notre-Dame de la Paix (FUNDP).

*matthieu.vandescuren@fundp.ac.be

[1] K. S. Novoselov, A. K. Geim, S. V. Morozov, D. Jiang, Y. Zhang, S. V. Dubonos, I. V. Grigorieva, and A. A. Firsov, Science **306**, 666 (2004).
[2] A. K. Geim and K. S. Novoselov, Nature Mater. **6**, 183 (2007).
[3] M. I. Katsnelson, Mater. Today **10**, 20 (2007).
[4] L. Tapasztó, G. Dobrik, Ph. Lambin, and L. P. Biró, Nat. Nanotechnol. **3**, 397 (2008).
[5] Y. Zhang, Y. W. Tan, H. L. Stormer, and Ph. Kim, Nature (London) **438**, 201 (2005).
[6] D. A. Abanin, P. A. Lee, and L. S. Levitov, Phys. Rev. Lett. **96**, 176803 (2006).
[7] K. Nomura and A. H. MacDonald, Phys. Rev. Lett. **96**, 256602 (2006).
[8] S. Bhattacharjee and K. Sengupta, Phys. Rev. Lett. **97**, 217001 (2006).
[9] F. Miao, S. Wijeratne, Y. Zhang, U. C. Coskun, W. Bao, and C. N. Lau, Science **317**, 1530 (2007).
[10] M. Fujita, K. Wakabayashi, K. Nakada, and K. Kusakabe, J. Phys. Soc. Jpn. **65**, 1920 (1996).
[11] K. I. Sasaki, J. Jiang, R. Saito, S. Onari, and Y. Tanaka, J. Phys. Soc. Jpn. **76**, 033702 (2007).
[12] M. Igami, M. Fujita, and S. Mizuno, Synth. Met. **103**, 2576 (1999).
[13] T. Tanaka, A. Tajima, R. Mariizumi, M. Hosoda, R. Ohno, E. Rokuda, C. Oshima, and S. Otani, Solid State Commun. **123**, 33 (2002).
[14] T. Yamamoto, K. Watanabe, and K. Mii, Phys. Rev. B **70**, 245402 (2004).
[15] D. W. Brenner, Phys. Rev. B **42**, 9458 (1990).
[16] J. Zhou and J. Dong, Appl. Phys. Lett. **91**, 173108 (2007).
[17] M. Yamada, Y. Yamakita, and K. Ohno, Phys. Rev. B **77**, 054302 (2008).
[18] D. W. Brenner, O. A. Shenderova, J. A. Harrison, S. J. Stuart, B. Nii, and S. B. Sinnott, J. Phys.: Condens. Matter **14**, 783 (2002).
[19] O. Shenderova, V. Zhirnov, and D. W. Brenner, Crit. Rev. Solid State Mater. Sci. **27**, 227 (2002).
[20] D. Sanchez-Portal, P. Ordejon, E. Artacho, and J. M. Soler, Int. J. Quantum Chem. **65**, 453 (1997).
[21] J. P. Perdew and A. Zunger, Phys. Rev. B **23**, 5048 (1981).

[22] N. Troullier and J. L. Martins, Phys. Rev. B **43**, 1993 (1991).
[23] E. Artacho, D. Sanchez-Portal, P. Ordejon, A. Garcia, and J. M. Soler, Phys. Status Solidi B **215**, 809 (1999).
[24] H. J. Monkhorst and J. D. Pack, Phys. Rev. B **13**, 5188 (1976).
[25] K. Parlinski, Z. Q. Li, and Y. Kawazoe, Phys. Rev. Lett. **78**, 4063 (1997).
[26] P. Hermet, J.-L. Bantignies, A. Rahmani, J.-L. Sauvajol, and M. R. Johnson, J. Phys.: Condens. Matter **16**, 7385 (2004).
[27] It has been shown that LDA and generalized gradient approximation (GGA) give similar results for phonon computation of graphite. In particular phonon frequencies have been calculated to be lower by 2% in GGA than in LDA [L. Wirtz and A. Rubio, Solid State Commun. **131**, 141 (2004)].
[28] J. Tersoff, Phys. Rev. Lett. **56**, 632 (1986).
[29] J. Tersoff, Phys. Rev. Lett. **61**, 2879 (1988).
[30] R. Al-Jishi and G. Dresselhaus, Phys. Rev. B **26**, 4514 (1982).
[31] C. Lanczos, J. Res. Natl. Bur. Stand. **45**, 255 (1950).
[32] K. Sbai, A. Rahmani, H. Chadli, J.-L. Bantignies, P. Hermet, and J.-L. Sauvajol, J. Phys. Chem. B **110**, 12388 (2006).
[33] H. Chadli, A. Rahmani, K. Sbai, P. Hermet, S. Rols, and J.-L. Sauvajol, Phys. Rev. B **74**, 205412 (2006).
[34] R. Haydock, V. Heine, and M. J. Kelly, J. Phys. C **8**, 2591 (1975).
[35] C. Benoit, E. Royer, and G. Poussigue, J. Phys.: Condens. Matter **4**, 3125 (1992).
[36] Q. Ding, Q. Jiang, Z. Jin, and D. Tian, Fullerene Sci. Technol. **4**, 31 (1996).
[37] This comparison method has already been used with defects in carbon nanotubes. M. Vandescuren, H. Amara, R. Langlet, and Ph. Lambin, Carbon **45**, 349 (2007).
[38] The recursion method is useful as a global method providing an overall view on phonon modes and allowing comparisons of the intensities of the peaks in VDOS spectra. However, when very precise characterizations are needed, the diagonalization method is the only alternative.
[39] The width of the ribbon is calculated without the C-H bond. Namely, it is the distance between the outmost carbons in the relaxed structure.